Cerebral Cortex January 2010;20:77-88
doi:10.1093/cercor/bhp080
Advance Access publication May 8, 2009

Number Processing Pathways in Human Parietal Cortex

Seppe Santens, Chantal Roggeman, Wim Fias and Tom Verguts

Department of Experimental Psychology, Ghent University, B-9000 Ghent, Belgium

Seppe Santens and Chantal Roggeman have contributed equally to this work.

Numerous studies have identified the intraparietal sulcus (IPS) as an area critically involved in numerical processing. IPS neurons in macaques are tuned to a preferred numerosity, hence neurally coding numerosity in a number-selective way. Neuroimaging studies in humans have demonstrated number-selective processing in the anterior parts of the IPS. Nevertheless, the processes that convert visual input into a number-selective neural code remain unknown. Computational studies have suggested that a neural coding stage that is sensitive, but not selective to number, precedes number-selective coding when processing nonsymbolic quantities but not when processing symbolic quantities. In Experiment 1, we used functional magnetic resonance imaging to localize number-sensitive areas in the human brain by searching for areas exhibiting increasing activation with increasing number, carefully controlling for non-numerical parameters. An area in posterior superior parietal cortex was identified as a substrate for the intermediate number-sensitive steps required for processing nonsymbolic quantities. In Experiment 2, the interpretation of Experiment 1 was confirmed with a connectivity analysis showing that a shared number-selective representation in IPS is reached through different pathways for symbolic versus nonsymbolic quantities. The preferred pathway for processing nonsymbolic quantities included the number-sensitive area in superior parietal cortex, whereas the pathway for processing symbolic quantities did not.

Keywords: fMRI, nonsymbolic, numerical cognition, numerical processing, symbolic

Introduction

Many animal species, from parrots to humans, are able to process number when presented in a nonsymbolic format (for recent reviews, see Dehaene et al. 1998; Brannon 2006). This suggests that number processing is biologically relevant and evolutionarily advantageous. Furthermore, the behavioral markers of this ability show striking correspondences between humans and nonhuman animals (e.g., distance and size effects, Dehaene et al. 1998). This close correspondence suggests that there are common species-independent constraints on the development of this ability and that the higher numerical skills in humans are rooted in this nonsymbolic numerosity system (Feigenson et al. 2004), the characteristics of which have recently begun to become uncovered.

Recent neuroscientific studies have described how neurons in the intraparietal sulcus (IPS) of human and nonhuman primates encode numerosity in a way that is consistent with the behavioral markers of numerical processing (Nieder and Miller 2004). Using single-cell recording in monkeys, trained in a match-to-numerosity task, Nieder et al. (2002) found neurons in the IPS and in the prefrontal cortex that responded to numerosity in a number-selective way (Nieder and Miller 2003). In particular, these neurons' firing rates were selectively tuned to a specific numerosity: It was maximal for its preferred numerosity, and the neural response "decreased" when the value of the presented numerosity was numerically more distant from the preferred numerosity.

Recent functional magnetic resonance imaging (fMRI) studies have confirmed the existence of a number-selective coding system in humans by means of the fMRI adaptation paradigm. Piazza et al. (2004, 2007) and Cantlon et al. (2006) showed neural adaptation for repeated numerosities and rebound of adaptation for deviant (i.e., numerically different) values in the anterior part of the IPS. In line with the tuning characteristics of the number-selective neurons described by Nieder et al. (2002), this rebound effect increased as the distance between the adaptation numerosity and the deviant numerosity increased (Nieder and Miller 2003). These adaptation effects were observed for numerosities (dot patterns; Piazza et al. 2004; Cantlon et al. 2006) as well as for symbolic numbers (Piazza et al. 2007).

The characteristics of the number-selective neurons can readily explain many aspects of overt behavior (Nieder and Miller 2004). However, not much is known about the neural processes leading up to activation of number-selective neurons; that is, the neural mechanisms that convert visual input, consisting of a symbol or a number of objects, into a number-selective code. In an attempt to bridge this gap, the systems that are required for this conversion have been investigated by computational modeling studies (Dehaene and Changeux 1993; Verguts and Fias 2004).

For the processing of nonsymbolic numerical input (sets of objects), these models proposed that 2 intermediate number-sensitive preprocessing steps are necessary for the conversion of visual input into a number-selective coding system. The first step is the creation of an object location map, a spatial neuronal map where each neuron signals the presence of an object at a given location, independent of the physical appearance of that object (Gottlieb 2007). Behavioral evidence for the contribution of such an object location map to the enumeration process derives from the fact that rapid enumeration of a small number of objects (i.e., subitizing) is only possible when the objects occupy different positions in space. When the to-be-enumerated objects are presented concentrically (i.e., objects at the same position in the object location map), subitizing is impossible and a counting procedure is required (Trick and Pylyshyn 1994). The object location map is number "sensitive" in the sense that when more objects are presented, more neurons will signal the presence of an object in its

receptive field, and consequently, there is more neural activity in the map as a whole. Note that the object location map, despite being number sensitive, is not number selective as it is not tuned to a specific numerosity.

After the object location map has been obtained from visual input, the information in this object location map must be further converted into a number-selective coding system. This conversion of the object location map into a number-selective coding system entails a nonlinear transformation (Verguts and Fias 2004). The most straightforward way to accomplish a nonlinear transformation in neural networks is to implement an intermediate preprocessing step between input and output. The nature of this intermediate step was investigated computationally (Verguts and Fias 2004). A neural network with an object location map as input was trained to construct a number-selective coding system at output. The network was equipped with an intermediate layer between input and output (for more details, see Verguts and Fias 2004). After training, it was found that neurons in this intermediate layer responded monotonously (i.e., monotonously stronger or weaker) when more objects were presented. Hence, the second preprocessing step between visual input and a number-selective coding system consisted of nodes accumulating or summating (in a positive or negative way) the number of objects that are activated in the first preprocessing step (the object location map). Therefore, this second preprocessing step was termed a summation coding system. The nodes in the summation coding system are number sensitive but, importantly, are not number selective because they do not selectively respond to a specific number.

Very recently, the biological reality of a summation coding system has been demonstrated by means of single-cell recording. Summation-type neurons have been discovered in the lateral intraparietal area (LIP) of the macaque monkey (Roitman et al. 2007). The responses of LIP neurons were recorded after presentation of a task-irrelevant visual array of 2, 4, 8, 16, or 32 elements. More than half of the recorded LIP neurons showed a monotonic relationship between firing rate and the number of elements presented to the neuron's receptive field, indicating that these neurons summated (in a positive or negative way) the number of elements displayed.

The computational modeling approach by Verguts and Fias (2004) is not restricted to nonsymbolic number processing. To simulate how initially arbitrary symbols can acquire numerical meaning by being associated with nonsymbolic numerosities during development, the model was presented simultaneously with nonsymbolic numerical input and the corresponding symbols. The latter were directly connected to the number-selective neurons because no nonlinearity is involved in the mapping from symbols to number-selective neurons. After training, it was observed that the number-selective neurons that were tuned to a specific numerosity also responded maximally to the corresponding symbolic input. Moreover, when symbolic input was given to the model, the number-selective neurons showed similar properties as when nonsymbolic input was presented, mirroring behavioral observations (Buckley and Gillman 1974; Koechlin et al. 1999). The model thus proposes that a number-selective coding system represents quantity regardless of the input format. However, this representation is accessed through different pathways. For nonsymbolic input, after preprocessing of the visual information in the object location map, a summation coding system is accessed before the number-selective representation. For symbolic input on the other hand, a direct pathway is possible without accessing the object location map and summation coding system.

At a behavioral level, evidence demonstrating the different processing of symbolic and nonsymbolic quantities has been found by Roggeman et al. (2007). They performed a priming study in which the effect of a briefly presented prime (Arabic digit or dot display) on the naming of a subsequently presented target number (Arabic digit or dot display) was evaluated. When primes were Arabic digits, a classic distance-dependent priming effect (faster naming of the target when the numerical distance between the prime and the target is small, see Reynvoet et al. 2002) was found. This distance-dependent priming effect provides evidence for access to the number-selective coding system. Indeed, because the tuning of number-selective neurons is not perfect, a prime number will not only activate neurons that are tuned to the prime's numerical value but will also activate neurons that are tuned to numerically close values, thereby facilitating the naming of subsequently presented numerically close numbers. In contrast, when primes were dot displays instead of numerical symbols, it was found that naming the target value was faster whenever the value of the prime was larger than or equal to the value of the target. This points to an underlying representation of numerosities in accordance with a summation coding system. In particular, if neurons respond more strongly with more objects, the neural code of the target will be sufficiently preactivated when the prime is larger than the target, which allows fast naming of the target. On the other hand, when the prime is smaller than the target, not all target neurons will be activated and additional neurons will have to be activated to name the target, increasing response time.

The aim of Experiment 1 is to locate brain regions that perform the number-sensitive preprocessing steps (object location map and summation coding system) that precede a number-selective coding system. In Experiment 2, we perform a connectivity analysis on separately acquired fMRI data to test whether the pathway for processing nonsymbolic number relies on the number-sensitive areas found in Experiment 1, whereas the pathway for symbolic numerical input does not.

Experiment 1

We presented dot displays containing 1–5 dots and measured neural activity for each numerosity. Numerosities were restricted to this range following our earlier studies (Roggeman et al. 2007) in which we provided behavioral evidence for summation coding. Stimuli were carefully constructed so that confounds of nonnumerical parameters (such as total luminance or object size) were eliminated. This was done in order to make sure that we would detect areas involved in "numerical" preprocessing steps (object location map and summation coding system) rather than areas that are sensitive to physical parameters that correlate with numerosity (see Materials and Methods).

Because number-sensitive neurons have been found in the monkey brain in area LIP (Roitman et al. 2007), we wanted to test if areas in the human parietal cortex that correspond functionally to monkey area LIP would also show number sensitivity. Based on the finding that LIP is involved in the execution of eye movements (Goldberg et al. 2002; Bisley and Goldberg 2003; Buschman and Miller 2007), participants were

engaged in a block design localizer run that consisted of a saccade task and a fixation task.

Materials and Methods

Participants

Twenty-one healthy adult volunteers were recruited from Ghent University and were paid for participation. Four participants were excluded from analysis due to poor performance (see Results). One other subject was excluded because of self-reported drowsiness. The remaining 16 participants (13 male, 1 left-handed male) were on average 22.2 years old (range: 19–26 years). All participants had normal or corrected-to-normal vision. All reported to have no neurological or psychiatric history. The study was approved by the ethical committee of the Medical Department of Ghent University. All participants gave written informed consent prior to scanning.

Stimuli

Stimuli were dot displays with a numerosity ranging from 1 to 5. The procedure to remove confounding effects of non-numerical parameters was based on Piazza et al. (2004) and Dehaene S, Izard V, Piazza M (unpublished data, 2005, available on www.unicog.org; see Fig. 1*A*). Nonnumerical parameters can be divided in intensive parameters (individual item size and interitem spacing) and extensive parameters (cumulative area of all dots in the display or total luminance, and total area spanned by the dot configuration). For a given numerosity, each intensive parameter is linearly related to one of the extensive parameters (Fig. 1*A*, linear relationship is shown as white lines for numerosities 1, 2, 3, 4, and 5). For example, when the numerosity is fixed and the size of the individual dots increases, the cumulative area of all dots also increases. Consequently, it is impossible to control both parameters simultaneously within a single pair of numerosities. The only way out is to use 2 pairs of numerosities, one controlling for the intensive parameters and the other for the extensive parameters. For this purpose, we constructed triplets of dot displays with increasing numerosity $n_{small} < n_{medium} < n_{large}$ (from now on referred to as n_s, n_m, and n_l, respectively). For the first pair of the triplet (n_s and n_m, yellow and magenta display in Fig. 1*A,B*), the intensive parameter (e.g., individual dot size) was constant (red line in the graph) but the extensive parameter (cumulative area of all dots) covaried congruently with numerosity: Cumulative area increased with increasing numerosity when individual dot size was constant. For the second pair (n_m and n_l, magenta and blue display in Fig. 1*A,B*), the extensive parameter was constant (purple line in the graph) but the intensive parameter covaried with numerosity. In this case, the covariance relation was incongruent because the individual dot size decreased with increasing numerosity when the cumulative area was fixed. Within the same triplet, the same logic was used for controlling the interitem spacing (intensive parameter) and total area spanned (extensive parameter). Thus, whereas both extensive parameters increase from n_s to n_m (and intensive parameters are constant), the intensive parameters decrease from n_m to n_l (and extensive parameters are constant), and numerosity is the sole parameter that monotonically increases from n_s to n_l. Therefore, brain areas that are found activated both in the contrast ($n_l > n_m$) and in the contrast ($n_m > n_s$; as measured by a conjunction analysis) can safely be regarded as areas responding solely to numerosity and not to the intensive or extensive confounding parameters. Note that the design is tailored to quantitatively distinguish neural responses to small, medium, and large numerosities (i.e., the categories n_s, n_m, and n_l) but does not allow distinguishing between individual numerosities because they could belong to multiple categories. Category n_s could be numerosity 1, 2, or 3, n_m could be numerosity 2, 3, or 4, and n_l could be numerosity 3, 4, or 5 (Fig. 1*B*). The stimuli in the separate localizer run were the displays for numerosity 1 used in the main experiment.

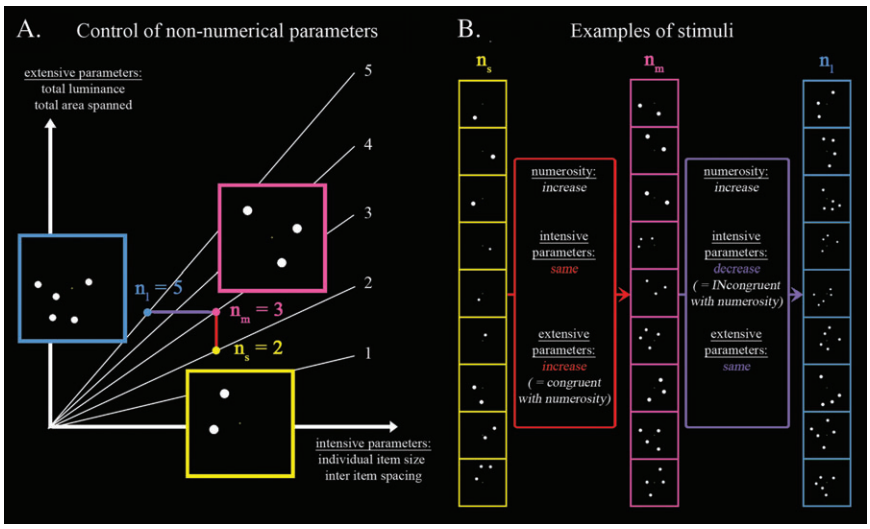

Figure 1. Control of nonnumerical parameters, as based on Piazza et al. (2004) and Dehaene S, Izard V, Piazza M (unpublished data). (*A*) Nonnumerical parameters were divided into intensive parameters (*x*-axis) and extensive parameters (*y*-axis). The linear relationship between these parameters for a given numerosity is schematically shown in the graph. Numbered lines specify this relationship for 1–5 dots. Colored lines provide an example of how stimuli were selected to remove the confounding influence of intensive or extensive parameter values. Starting from a medium numerosity (n_m), a smaller numerosity (n_s) is selected with the same intensive parameter and a larger numerosity (n_l) with the same extensive parameter. In this way, only numerosity increases from n_s over n_m to n_l (for details, see text). (*B*) Examples of stimuli with different numerical values in the categories n_s, n_m, and n_l.

Dot displays were generated randomly by an adapted version of a Matlab program (Matlab 7.0.4, The MathWorks, Inc., Natick, MA) described in Dehaene S, Izard V, Piazza M (unpublished data). Dots were displayed in an area of approximately 10 × 10 visual degrees. The minimum and maximum item size varied between 0.2 and 0.63 visual degrees. Further details about the generation of the dot displays are given in the Supplementary Material.

Experimental Procedure

Stimuli were presented for 150 ms, white against a black background. A small yellow fixation cross remained on the screen throughout the total scan time, and participants were instructed to fixate the cross during the whole scan session. Stimuli were presented on average every 5 s, with a jittering factor (Burock et al. 1998; Dale 1999; Miezin et al. 2000) varying between 0 and 1600 ms, so that the interstimulus interval between 2 consecutive events could vary between 3400 and 6600 ms. In all, 20% of all events were null events. In order to make sure that participants paid attention to the stimuli, occasionally (on 12% of all events), a task trial was introduced. In these task trials, 2 Arabic digits were presented left and right of fixation, and participants were asked to indicate the number corresponding to the numerosity of the previous dot display by pressing a button with their left or right index finger (for a snapshot of the experimental design, see Fig. 2). The experiment consisted of 5 runs with 102 events per run. Order of the 5 event types (n_s, n_m, n_l, null events, and task trials) was pseudorandomly intermixed with first-order counterbalancing within runs (each trial type followed every other trial type equally often; Dale and Buckner 1997; Buckner et al. 1998). Order of numerosities 1, 2, 3, 4, and 5 was counterbalanced over all runs for each subject.

In the localizer run, every stimulus was presented for 1 s and was immediately followed by another stimulus, yielding a dot that changed location and size every second. During the saccade blocks, participants were asked to make a saccade to the dot and back to the fixation cross every time the dot changed position.

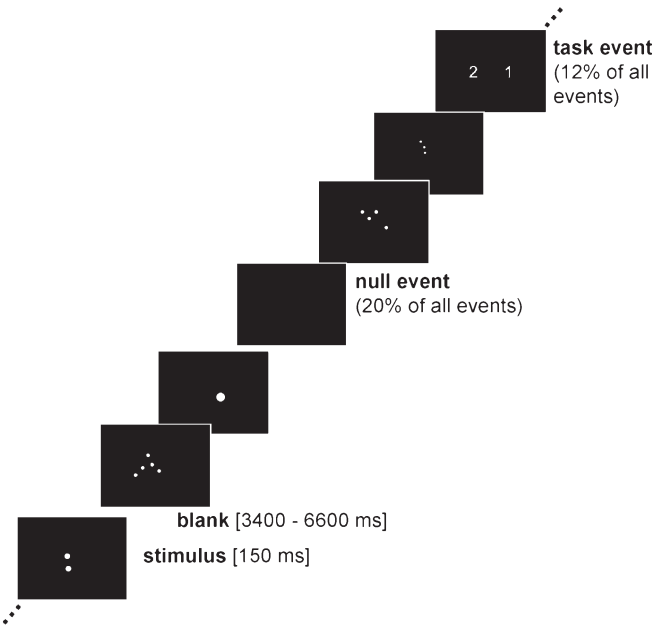

Figure 2. Experiment 1. Snapshot of the experimental design.

During the fixation blocks, participants were asked to ignore the dots and to keep fixating the fixation cross. The task was indicated by the color of the fixation cross (red: make saccades, yellow: no saccades). Block duration was 16 s. The saccade and fixation block alternated, and each block was repeated 8 times. In all, 135 images were acquired with the same echo planar imaging (EPI) sequence as the main experiment.

The experimental procedure was controlled with E-Prime 1.1 SP3 (www.pstnet.com/eprime; Psychology Software Tools). Stimuli were presented through dual display MRI compatible LCD displays and mounted in a lightweight headset (VisuaStim XGA, Resonance Technology Inc., Northridge, CA; http://www.mrivideo.com/).

Imaging Procedure

Participants were positioned head first and supine in the bore. Images were collected with a 3T Magnetom Trio MRI scanner system (Siemens Medical Systems, Erlangen, Germany), using an 8-channel radio frequency head coil. First, 176 high-resolution anatomical images were acquired using a T_1-weighted 3D anatomical sequence (time repetition [TR] = 1550 ms, time echo [TE] = 2.89 ms, image matrix = 256 × 256, field of view [FOV] = 220 mm, flip angle = 9°, slice thickness = 0.9 mm, voxel size = 0.9 × 0.871 × 0.871 mm [resized to 1 × 1 × 1 mm], 176 sagittal slices). Whole-brain functional images were collected using a T_2^*-weighted EPI sequence, sensitive to blood oxygen level–dependent (BOLD) contrast (TR = 2000 ms, TE = 30 ms, image matrix = 64 × 64, FOV = 224 mm, flip angle = 90°, slice thickness = 3.0 mm, distance factor = 17%, voxel size 3.5 × 3.5 × 3 mm, 31 axial slices). In all, 256 images were acquired per run.

Image Processing and Statistical Analysis

Data analysis was performed using the SPM5 toolbox (http://www.fil.ion.ucl.ac.uk/spm/). An unforeseen technical problem caused inaccurate timing of events in the first run. Therefore, the first run was discarded from the analyses for all participants. Functional volumes were corrected for slice timing, motion corrected to the first image of each run (second degree B-spline interpolation). Next, the combined tissue classification, bias correction, and nonlinear warping procedure of SPM5 were used to normalize the functional and anatomical images to the Montreal Neurological Institute (MNI) template. Functional images were smoothed with a Gaussian kernel of 8-mm full-width half maximum (FWHM) prior to statistical analysis.

Functional data were subjected to a general linear model (GLM) analysis with 5 predictors per session (n_s, n_m, n_l, response left, and response right). The protocol was specified in milliseconds and convolved with the canonical hemodynamic response function. Six extra predictors derived from the realignment procedure modeled head motion. The data were high-pass filtered with a cutoff of 120.5 s. For multisubject GLM, runs of the same subject were implemented as fixed effects, between subjects as random effects. Conjunction of the 2 contrasts of interest ($n_l > n_m$) and ($n_m > n_s$) was calculated based on the minimum *t*-statistic compared against the conjunction null (Nichols et al. 2005). To ensure sufficient sensitivity with this very conservative procedure (Friston et al. 2005), our results are based on activations at a P level of 0.005 with a cluster extent threshold of 20 voxels. Results with a statistical threshold of $P < 0.001$ are reported briefly.

Results

Behavioral Results

Four participants were excluded due to poor performance on the task trials, suggesting that they did not attentively process the stimuli. We excluded participants when they made more than 20% errors over the 4 runs or when they made more than 30% errors in a single run. The remaining participants made on average 6.25% errors (range: 0–7 errors on the total of 48 trials).

Whole-Brain Analysis

The whole-brain random effects analysis of the conjunction ($n_l > n_m$) and ($n_m > n_s$) yielded a network of bilateral occipital and parietal areas and an area in the medial frontal gyrus (see Fig. 3).

Occipital activation was found in the right lingual gyrus (MNI coordinates: 14, –88, –3, 20 voxels). Activations in the middle occipital gyrus were centered left around (–32, –88, 18 [113 voxels]) and right around (39, –81, 15 [93 voxels]) but extended in lateral and inferior directions, thus overlapping with regions identified as area lateral occipital complex (LOC) (Grill-Spector et al. 1998; Tootell and Hadjikhani 2001; Denys et al. 2004). The activation in the medial frontal gyrus (–4, 18, 42, 35 voxels) was situated in an area generally recognized as pre-SMA (Behrens et al. 2006; Klein et al. 2007). Significant clusters of activations (left: –21, –60, 54, 44 voxels; right: 21, –63, 63, 37 voxels) were also found symmetrically in the posterior part of the superior parietal lobe (see Fig. 3*A,B*, also Fig. 3*D,E*). All clusters survived a threshold for the conjunction of $P < 0.001$ (uncorrected for multiple comparisons; right lingual gyrus: 5 voxels; left middle occipital gyrus: 59 voxels; right middle occipital gyrus: 33 voxels; medial frontal gyrus: 6 voxels; left posterior superior parietal lobe: 13 voxels; and right posterior superior parietal lobe: 8 voxels).

Region of Interest Analysis

We computed the contrast saccade versus fixation on the images of the localizer run, thresholded at $P < 0.05$ with a false discovery rate correction. We then selected in both hemispheres the active voxels in a sphere with radius 12 mm around the local maximum that corresponded with coordinates of a human homologue of LIP as reported in the literature (Sereno et al. 2001; Simon et al. 2002; Koyama et al. 2004). The left hemisphere human LIP region of interest (ROI) was centered at –11, –63, 63; the right hemisphere human LIP ROI was

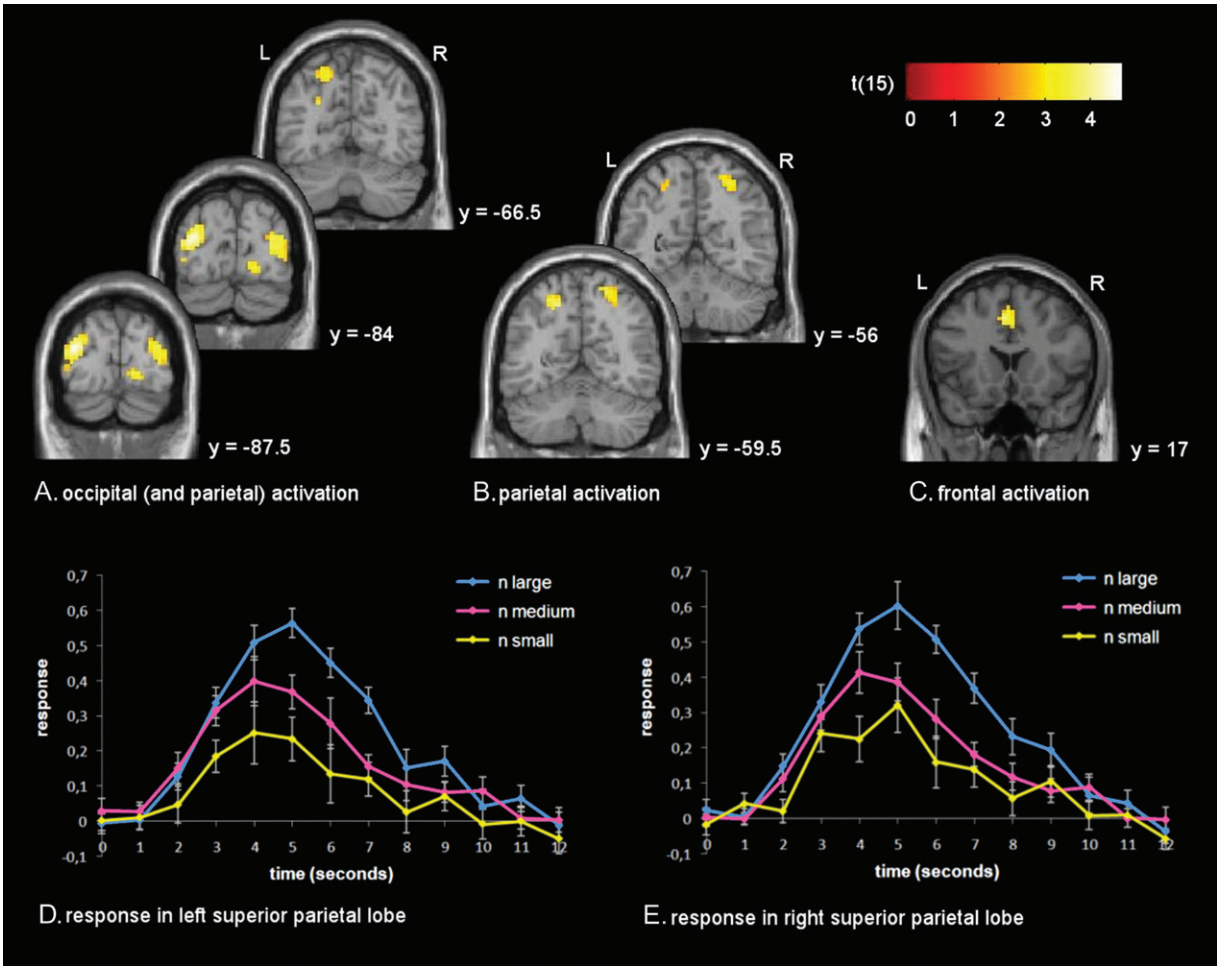

Figure 3. Experiment 1, results of the random effects analysis of the conjunction ($n_l > n_m$) and ($n_m > n_s$). For MNI coordinates, see text. (*A*) Activation in bilateral middle occipital gyrus, right lingual gyrus, and left inferior occipital gyrus. Activation in the left superior parietal lobe is also visible. (*B*) Activation in posterior part of the superior parietal lobe. (*C*) Activation in pre-SMA. (*D*) Poststimulus time histogram for the area in the left superior parietal lobe. (*E*) Poststimulus time histogram for the area in the right superior parietal lobe.

centered at 21, –63, 57. The ROIs of human LIP were adjacent to and partly overlapping with the areas found active in the random effects whole-brain analysis. The left ROI was situated slightly more superior and medial than the random effects activation; the right ROI was situated slightly more posterior and medial.

Given that the ROIs did not completely overlap with the whole-brain activation for the conjunction, we tested if the ROIs were also number sensitive. The random effects analysis on the average activation over all voxels in these ROIs showed that the conjunction ($n_l > n_m$) and ($n_m > n_s$) was significant for the ROI in both hemispheres (left: $t_{15} = 1.90$, $P < 0.05$; right: $t_{15} = 1.90$, $P < 0.05$).

Discussion

The goal of Experiment 1 was to detect and localize number-sensitive areas in the human brain. The results showed a network of bilateral occipital and parietal areas and an area in the medial frontal gyrus. Given that Roitman et al. (2007) found summation coding neurons in monkey area LIP, we wanted to assess the potential analogy of nonsymbolic number processing in the monkey and the human brain. The ROI analysis showed number sensitivity in bilateral posterior superior parietal areas that functionally correspond to monkey LIP. This suggests that the superior parietal cortex houses the neural substrate for number-sensitive coding systems in humans.

A number of alternative interpretations for the positive correlation between the number of dots and the BOLD signal in this area can be ruled out. The number-sensitive activation observed in this study could not be due to response selection because the task was only occasionally and unpredictably inserted after a dot pattern stimulus and was always to choose between 2 Arabic digits. Moreover, the task was implemented as separately defined task trials and was modeled separately, so number-sensitive activation cannot be confounded with activation due to response selection.

One could argue that the positive relation between number of dots and neural activity in the ROI analysis reflects the fact that there was more saccade-related processing when participants were presented with displays containing more dots. Several arguments can be raised against this interpretation. Stimuli were presented for a duration of only 150 ms, which is too short to allow programming and executing even one saccade, let alone a number of saccades as a function of numerosity. Still, one could maintain that not the actual execution of saccades but the mere intention to make a saccade is sufficient to activate the saccade area defined by the localizer task. However, Connolly et al. (2002) convincingly demonstrated that the human homologue of LIP, contrary to the frontal eye fields (FEFs), was not activated by saccadic intention alone. Indeed, whereas the FEFs were activated during the planning period preceding a saccade, human LIP was only activated when the saccade target appeared and the saccade was actually executed. This study thus suggests that the absence of FEF activity in our conjunction analysis makes it unlikely that participants planned more saccades when more dots were presented. Even if more saccades were planned, this could not have led to an increased BOLD response in the superior parietal areas. Moreover, Lee et al. (2006) presented several possible saccade target stimuli, varying the number of potential saccade target locations. A positive correlation between the strength of the BOLD response and number of target locations was observed in the IPS only when an actual saccade target was selected and the saccade was effectively executed. Together, these studies rule out an interpretation in terms of the number of saccades that is planned for a particular stimulus. Finally, Todd and Marois (2004) found neural activity in the IPS to be correlated with the number of elements in a visual display during encoding and active maintenance in visual short-term memory. In a control condition without the need to maintain the visual objects in memory, parietal activity was not modulated by the number of objects displayed. The areas found by Todd and Marois could be the same as the ones we found. The task used by these authors would indeed activate an object location map, which may be involved in visuospatial working memory. Nevertheless, the Todd and Marois study does not allow concluding that the posterior superior parietal is number sensitive because in their study nonnumerical physical parameters were not controlled.

In addition to superior parietal cortex, also occipital and frontal areas were found to be number sensitive in Experiment 1. To further investigate the functional properties of these different areas, Experiment 2 was set up.

Experiment 2

As discussed in the Introduction, the model of Verguts and Fias (2004) assumes a number-selective representation that is shared for symbolic and nonsymbolic number. This number-selective representation has been previously associated with IPS (for reviews, see Dehaene et al. 2003; Cohen Kadosh et al. 2008). The model proposes that this shared representation is reached through 2 different pathways. For nonsymbolic quantities, the pathway should include areas that perform the number-sensitive preprocessing steps (object location map and summation coding), whereas the pathway for symbolic quantities does not depend on these areas. Based on the ROI analysis of Experiment 1, we suggested that the superior parietal areas would house these number-sensitive preprocessing steps. If this is correct, the pathway from early visual areas (where both symbolic and nonsymbolic numbers are initially processed) to this superior parietal area and from the latter area to number-selective areas in IPS should be stronger for nonsymbolic than for symbolic numbers. In contrast, the pathway from the early visual areas directly to number-selective areas should be stronger for symbolic numbers. This is tested in Experiment 2 with an effective connectivity analysis using structural equation modeling (STM).

Besides the superior parietal areas, Experiment 1 also indicated occipital and frontal areas as number sensitive. The functional properties of these areas were explored by subjecting them to the same connectivity analysis. If these areas are not involved in number processing, a different connectivity pattern should emerge when they replace the superior parietal area in the SEM.

Materials and Methods

Participants

Twelve healthy adult volunteers (all male, right-handed) were recruited from a student pool at Ghent University and were

paid for participation. None of them had participated in Experiment 1. The participants had a mean age of 19.9 (range: 19–23 years). All had normal or corrected-to-normal vision and reported to have no neurological or psychiatric history. The study was approved by the ethical committee of the Medical Department of Ghent University. All participants gave written informed consent prior to scanning.

Stimuli

The experiment consisted of a block design with blocks of nonsymbolic quantities (dot patterns), blocks of symbolic quantities (Arabic digits), and fixation blocks. During blocks of nonsymbolic stimuli, dot displays were presented with a numerosity ranging from 1 to 5. These stimuli were constructed using the same routines as in Experiment 1. In the first half of the experiment, the values for 2 of the 4 nonnumerical parameters (individual item size, interitem spacing, cumulative area, and total area spanned by the dot configuration; Dehaene S, Izard V, Piazza M, unpublished data; Piazza et al. 2004) were drawn from a fixed distribution, regardless of the number of dots, whereas the 2 other nonnumerical parameters necessarily correlated with numerosity. In the second half of the experiment, 2 other parameters were drawn from a fixed distribution and the other 2 again correlated with numerosity. All combinations of controlled parameters occurred equally often over the 12 participants. The displays spanned maximally 7.8 visual degrees, both horizontally and vertically. Blocks of symbolic stimuli consisted of Arabic digits ranging from 1 to 5, printed in Courier font. The digits spanned about 2.8 visual degrees horizontally and 4 degrees vertically, which corresponded to the mean cumulative area of the dot displays.

Experimental Procedure

A small light blue fixation cross remained in the center of the screen throughout the total scanning time, and participants were instructed to fixate the cross during the whole scan session. Stimuli were centered around this fixation cross, white against a black background. A stimulus was presented for 200 ms, every 1150 ms. There were 10 blocks of symbolic stimuli and 10 blocks of nonsymbolic stimuli. After blocks 4, 8, 12, and 16, a fixation block was introduced, during which participants had to maintain fixation on the fixation cross for 16 100 ms. In order to ensure sustained attention to the stimuli, a task was presented at the end of each block (see Fig. 4). In this task, 2 stimuli were presented left and right of the fixation cross, and participants were asked to indicate the number corresponding to the previous display by pressing a button with their left or right index finger. 4000 ms after the presentation of the 2 task stimuli, a new block started, synchronized with the beginning of the next TR. Blocks had a variable length and consisted of 13 (14 950 ms) to 27 stimuli (31 050 ms). Blocks of symbolic and nonsymbolic stimuli alternated randomly. All blocks were presented within one scanning session. Over the whole scanning session, 200 symbolic and 200 nonsymbolic stimuli were presented.

The experimental procedure was controlled using the Tscope library for the C programming language (Stevens et al. 2006). Stimuli were presented on a back-projection screen at the head of the scanner bore. Participants viewed the screen through a mirror mounted on the head coil.

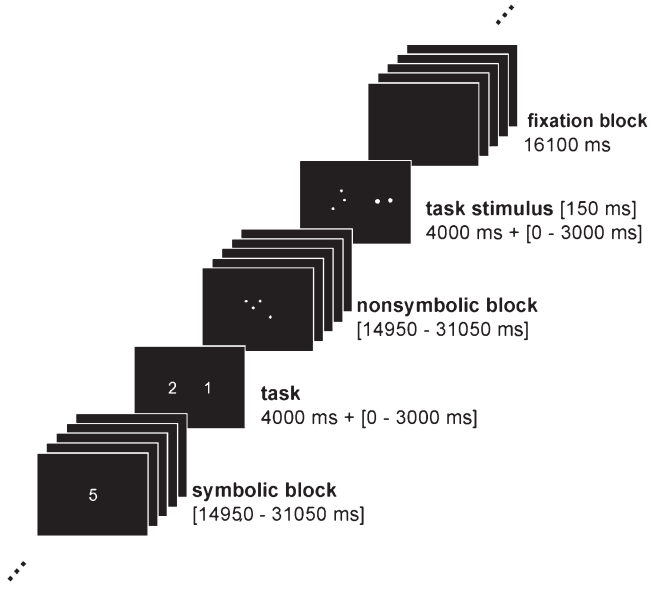

Figure 4. Experiment 2. Snapshot of the experimental design.

Imaging Procedure

Participants were positioned head first and supine in the bore. Images were collected using the same MRI scanner and head coil as in Experiment 1. A 3D high-resolution T_1-weighted anatomical image was first acquired for coregistration with the functional images, using the same anatomical sequence as in Experiment 1. Whole-brain functional images were acquired using a T_2^*-weighted EPI sequence, sensitive to BOLD contrast (TR = 3000 ms, TE = 33 ms, image matrix = 64 × 64, FOV = 192 mm, flip angle = 90°, slice thickness = 3.0 mm, distance factor = 33%, voxel size 3 × 3 × 3 mm, 46 axial slices). In all, 228 functional volumes were acquired during the functional scanning session.

Image Processing and Statistical Analysis

Data analysis was performed using the SPM5 toolbox (http://www.fil.ion.ucl.ac.uk/spm/). Functional volumes were corrected for slice timing, motion corrected to the middle volume of the session (second degree B-spline interpolation), and coregistered to the anatomical volume. Next, the combined tissue classification, bias correction, and nonlinear warping procedure of SPM5 were used to normalize the functional and anatomical images to the MNI template. Functional images were smoothed with a Gaussian kernel of 8-mm FWHM prior to statistical analysis.

Functional data were subjected to a GLM analysis with 3 predictors describing the experimental design (symbolic, nonsymbolic, and task). The protocol was specified in milliseconds and convolved with the canonical hemodynamic response function. Six extra predictors derived from the realignment procedure modeled head motion. The data were high-pass filtered with a cutoff of 128 s. For the purpose of defining representative time series (see below), statistical maps were created for each participant for the contrast nonsymbolic > symbolic and for the conjunction between symbolic and nonsymbolic. For multisubject GLM, runs of the same subject were implemented as fixed effects, between subjects as random effects. Conjunctions were calculated based

on the minimum *t*-statistic compared against the conjunction null (Nichols et al. 2005). As in Experiment 1, activations are reported at a *P* level of 0.005 with a cluster extent threshold of 20 voxels.

The second-level analysis of the imaging results showed shared activation for symbolic and nonsymbolic stimuli in the left IPS but not in the right IPS (see below). Therefore, the number-selective areas analysis was restricted to areas in the left hemisphere. To obtain the data for this analysis, we computed the first eigenvariate time series of the areas we were interested in for each participant separately: early visual areas, number-sensitive areas, and number-selective areas (see Fig. 5). For early visual areas, the time series were computed over the voxels of Brodmann area 17 as defined by the WFU Pickatlas tool (Maldjian et al. 2003). To avoid an excessive amount of noise, voxels were excluded that did not survive a liberal threshold of $P < 0.05$ (uncorrected) for the conjunction of symbolic and nonsymbolic formats on the participant level. For number-selective areas, the time series were computed over the voxels of the left parietal area that was activated in the second-level conjunction analysis of Experiment 2. Again, voxels were excluded that did not survive the $P < 0.05$ level for the conjunction of symbolic and nonsymbolic formats on the participant level. Because Experiment 1 suggested different candidates for number-sensitive areas, we performed 3 different number-selective areas analyses. Although keeping the data for early visual areas and number-selective areas the same, the data for number-sensitive areas were different for each of these analyses. The first eigenvariate time series for number-sensitive areas were computed, respectively, over the voxels of the superior parietal, the middle occipital, and the pre-SMA areas that were activated in the second-level conjunction analysis of Experiment 1. Voxels were excluded that did not survive the $P < 0.05$ (uncorrected) level for the contrast nonsymbolic > symbolic on the participant level. Participants with no activated voxels above the $P < 0.05$ threshold for one of these regions were excluded from the analyses for this region. One participant was excluded this way for the analysis with the data for number-sensitive areas extracted from the superior parietal area, 3 participants

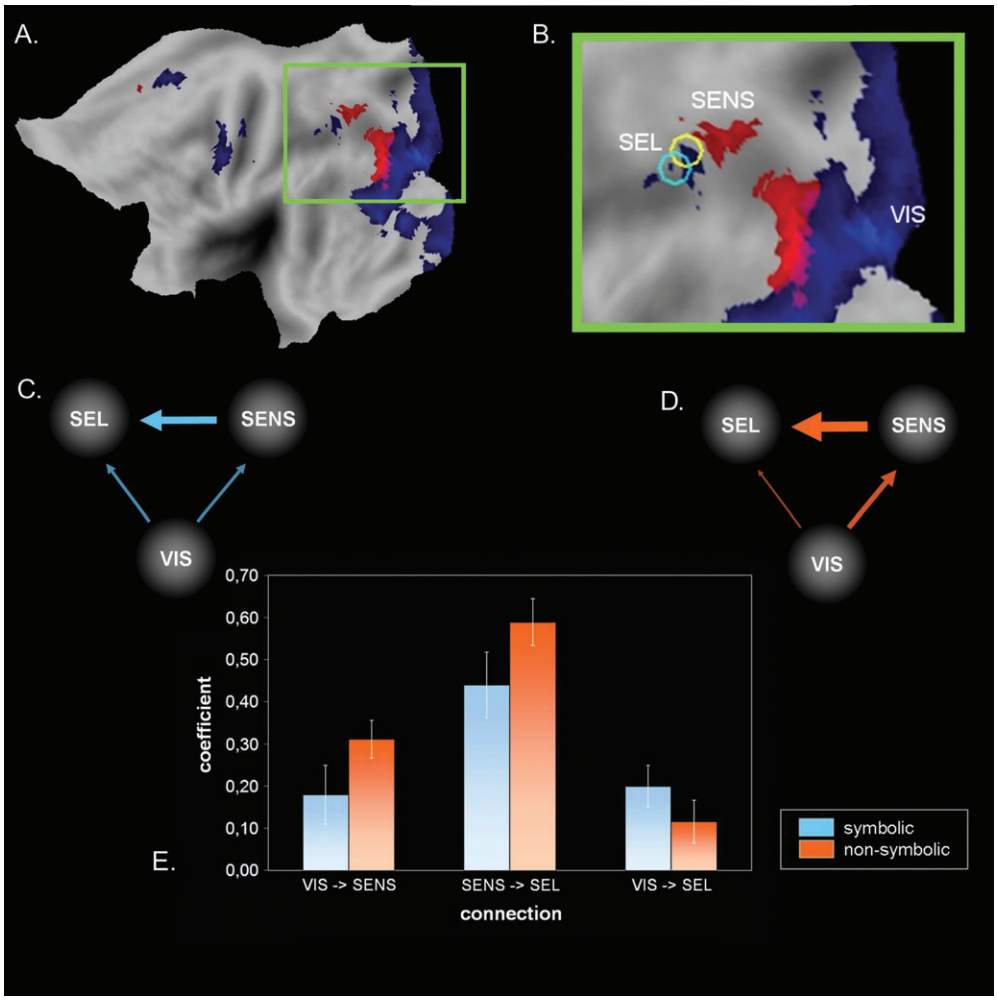

Figure 5. (*A*, *B*) Activation from the random effects analyses of Experiments 1 and 2, mapped onto population-averaged human brain by Caret (http://brainvis.wustl.edu/wiki/index.php/Caret:About, Van Essen and Drury 1997). In red, the conjunction ($n_l > n_m$) and ($n_m > n_s$) of Experiment 1; in blue, the conjunction symbolic and nonsymbolic of Experiment 2. The yellow ring represents the overall mean coordinates obtained from the meta-analysis by Cohen Kadosh et al. (2008). The cyan ring represents the left parietal peak activation for regions showing a distance-dependent recovery from adaptation as found by Piazza et al. (2007). VIS: primary visual region (for precise definition, see text). SENS: number-sensitive region in the superior parietal lobe. SEL: number-selective region in IPS. (*C*, *D*) Graphical representation of the SEM for symbolic (*C*) and nonsymbolic (*D*) blocks (line weight correlates with path coefficient). (*E*) Path coefficients resulting from the SEM analysis for different connections and different formats.

for the analysis with the data from the middle occipital area, and 2 participants for the analysis with the data from pre-SMA.

The same procedure was followed for each of the 3 SEM analyses. First, for each of the 3 extracted time series (early visual areas, number-sensitive areas, and number-selective areas), we separated the data of symbolic and nonsymbolic blocks into 2 vectors. The 6 resulting vectors were normalized (zero mean, unit variance) and were then used to construct 2 covariance matrices, one for the data from the symbolic blocks and one for the data from the nonsymbolic blocks. This way, 12 unique data points {2 [symbolic and nonsymbolic] × [3 (variances) + 3 (covariances)]} were obtained per analysis for each participant. For the number-selective areas analysis, a model was designed with the same structure for the symbolic and the nonsymbolic data. Unique variances were allowed for early visual areas, number-sensitive areas, and number-selective areas, and forward connections were assumed between these 3 areas: from early visual areas to number-sensitive areas, from number-sensitive areas to number-selective areas, and from early visual areas to number-selective areas (see Fig. 5). First, we ensured that it was meaningful to assume different path coefficients for symbolic and nonsymbolic formats. To this end, a null model in which connections were restricted to be equal for the 2 different formats was compared with a full model that allowed different path coefficients for different formats (for a similar approach, see Büchel and Friston 1997). Each model was fitted for each participant separately, and the null hypothesis of no differences between stimulus formats was tested with a chi-square statistic. To obtain a test over all 12 participants, the test statistics (each chi square distributed with 3 degrees of freedom) were added across participants (Christensen 2002). Next, the path coefficients of the full model were entered in a random effects analysis to test our specific predictions at the population level.

Results

Behavioral Results

Due to a technical malfunction, the behavioral data of one participant were not correctly registered. The mean accuracy of the other 11 participants on the 1-back task was 82%. There was a significant difference in mean reaction time on the correct trials for symbolic stimuli (577 ms) and for nonsymbolic stimuli (785 ms; $F_{1,10} = 32.55$, $P < 0.001$).

Whole-Brain Results

The results of the second-level conjunction between symbolic and nonsymbolic blocks are shown in blue in Figure 5. Not surprisingly, viewing symbolic and nonsymbolic stimuli activated a widespread network of visual areas in the bilateral occipital cortex. Activation was also found in left and right central and precentral gyrus and in pre-SMA. Finally, the conjunction also revealed activation in the left parietal lobe. A cluster of 59 voxels was located in the IPS, with the local maximum at –36, –60, 57. This is very close to the activation peaks that show a distance effect in recovery from adaptation, regardless of stimulus format (Piazza et al. 2007). The location of the left parietal peak also corresponds very well to the average coordinates reported in a recent meta-analysis of studies on numerical cognition (Cohen Kadosh et al. 2008; see Fig. 5).

SEM Results

The SEM analyses were performed 3 times, with the data for number-sensitive areas extracted from the superior parietal, the middle occipital, and the medial frontal areas found in the conjunction analysis of Experiment 1. When the time series for number-sensitive areas were extracted from the superior parietal area, the full model with different path coefficients for symbolic and nonsymbolic formats fitted significantly better than the model with equal path coefficients ($\chi^2(36) = 56.19$, $P < 0.05$). All path coefficients of the full model were significantly higher than zero at a P level of 0.05 (1-tailed). These path coefficients were compared across stimulus formats using an analysis of variance (ANOVA) with a 2 (format: symbolic or nonsymbolic) by 3 (connection: early visual areas to number-sensitive areas, number-sensitive areas to number-selective areas, or early visual areas to number-selective areas) design. There was a main effect of format ($F_{1,10} = 8.19$, $P < 0.05$): path coefficients for nonsymbolic paths were higher than for symbolic paths. There was also a main effect of connection ($F_{2,20} = 10.63$, $P < 0.01$). Importantly, the interaction between format and connection was significant: $F_{2,20} = 8.89$, $P < 0.01$. We used 1-tailed planned comparisons to test our predictions in more detail. The path coefficients for the connections between early visual areas and number-sensitive areas and between number-sensitive areas and number-selective areas were greater for nonsymbolic than for symbolic quantities ($t_{10} = 3.31$, $P < 0.01$; $t_{10} = 4.19$, $P < 0.001$, respectively), whereas the coefficients for the connection between early visual areas and number-selective areas were close to significantly stronger for the symbolic than for the nonsymbolic format ($t_{10} = 1.67$, $P = 0.063$; see Fig. 5, panel *E*).

In the analyses with the time series for number-sensitive areas extracted from the middle occipital gyrus, the full model was not significantly better than the null model with equal path coefficients for symbolic and nonsymbolic formats ($\chi^2[27] = 35.84$, $P = 0.119$). The path coefficients of the full model were significantly higher than zero, except for the coefficient of the path between early visual areas and number-selective areas in the nonsymbolic blocks. The ANOVA on the path coefficients of the full model showed no main effect for format ($F_{1,8} = 0.380$, $P = 0.56$). There was a main effect of connection ($F_{2,16} = 5.16$, $P < 0.05$). There was no significant interaction between format and connection ($F_{2,16} = 0.717$, $P = 0.50$; see Supplementary Fig. S1, panel *A*).

When the time series for number-sensitive areas were extracted from the pre-SMA, the model with different path coefficients for symbolic and nonsymbolic formats was significantly better than the model with equal path coefficients ($\chi^2[30] = 57.78$, $P < 0.01$). The path coefficients of the full model were significantly higher than zero, except for the coefficient of the path between early visual areas and number-sensitive areas in the symbolic blocks. Importantly, there were no main effects of format and connection ($F_{1,9} = 1.60$, $P = 0.238$ and $F_{2,18} = 2.73$, $P = 0.092$, respectively) nor was there an interaction between these factors ($F_{2,18} = 0.91$, $P = 0.422$; see Supplementary Fig. S1, panel *B*).

Discussion

In Experiment 2, we further investigated the functional properties of the different number-sensitive areas that were found in Experiment 1. To this end, we performed a functional

connectivity analysis using SEM. It was confirmed that an area in the left IPS to which the number-selective representation of quantity has been ascribed shows a different functional connectivity with visual and number-sensitive areas for symbolic versus nonsymbolic quantities. We showed that processing nonsymbolic quantities relies on a pathway that includes an area in the left parietal cortex, medial, and posterior to the areas that have been shown to be activated by a number-selective coding system. Processing symbolic quantities on the other hand relies more on a pathway that does not include this posterior superior parietal activation.

When fitting the SEM to the data for number-sensitive areas extracted from the occipital area found in Experiment 1, there was no evidence that they are part of a pathway for processing nonsymbolic numerical stimuli. We therefore provide possible explanations why the strength of the BOLD response in these areas correlated with numerosity in Experiment 1. Notwithstanding the careful control of intensive and extensive variable such as area, dot size, luminance, and interdot spacing, it is still possible that displays with few dots have different visual properties than displays with more dots. As an example, displays containing more dots are visually more complex, even when intensive and extensive variables are controlled. Interestingly, the visual areas that were modulated by numerosity comprised the LOC. A number of studies have demonstrated the involvement of LOC during the perception of illusory contours (for a review, see Seghier and Vuilleumier 2006). This suggests that the visual system tries to derive shape by connecting individual visual elements. This is consistent with Murray et al. (2004) who found higher activation in LOC when visual perception involved grouping of individual elements into a coherent representation. The lingual gyrus, where we also observed a positive correlation between the BOLD signal and numerosity, has also been implied in the perception of illusory contours (Halgren et al. 2003). It can therefore be argued that the involvement of lingual gyrus and the middle occipital gyrus in our study reflects the mandatory tendency of the visual system to construct visual patterns. Indeed, within our range of low numerosities, the perceptual organization of 2 dots as a line, 3 dots as a triangle, and 4 dots as a quadrangle is quite salient. Importantly, earlier behavioral studies have ruled out the tendency to perceive shapes in visual dot displays as a critical factor for rapid enumeration (subitizing) of visual dot displays (Trick and Pylyshyn 1994). Together with absence of an interaction between input format and processing pathway, we conclude that the observed modulation of occipital areas by numerosity is not a critical numerical preprocessing step but is a mere side effect of the way the visual system operates.

Activation that positively correlated with numerosity in Experiment 1 was also found in pre-SMA. However, the ANOVA on the path coefficients from the number-selective areas analysis of Experiment 2 showed no main effects nor an interaction between format and connection. The exact reason for the pre-SMA activation in Experiment 1 remains unclear, but it is safe to assume that pre-SMA does not reflect the type of number-sensitive preprocessing that is required to convert visual numerosity into a number-selective coding system because it is not located in the occipitoparietal stream of visual information. It is more likely that pre-SMA receives numerical information that has been computed at earlier stages of the cortical hierarchy (for a similar argument, see also Nieder 2005). Possibly, an interaction between numerical processing and intended action as evidenced by some authors (Badets et al. 2007; Moretto and di Pellegrino 2008) might have caused activation in pre-SMA. The precise reasons for its involvement remain to be found out.

General Discussion

In this study, we identified an area in the posterior superior parietal cortex as the neural substrate for a number-sensitive coding system in humans. In Experiment 1, areas were localized that showed an increase in BOLD signal with increasing numerosity, while tightly controlling for different visual parameters. In Experiment 2, we investigated the functional connectivity of these areas. It was shown that only the functional connectivity pattern of the posterior superior parietal area found in Experiment 1 agreed with the model architecture proposed by Verguts and Fias (2004). Based on a series of computational modeling simulations, these authors suggested 2 separate processing pathways for symbolic and nonsymbolic quantities. Roggeman et al. (2007) already supported this idea with behavioral experiments. The results from Experiment 2 provide converging neural evidence for this idea. Both electrophysiological (Nieder and Miller 2004) and neuroimaging studies (Piazza et al. 2004, 2007; Cantlon et al. 2006) have indicated an area in the IPS as the neural substrate for a number-selective representation of number. Piazza et al. (2007) showed that this representation is shared for both symbolic and nonsymbolic studies. In the whole-brain analysis of Experiment 2, we confirm that a portion of the IPS is activated by numerical stimuli, regardless of the input format. However, the number-selective areas analysis showed that the different pathways to reach this area are modulated by the input format. For nonsymbolic quantities, the pathway that includes the number-sensitive area in posterior superior parietal cortex is stronger. In contrast, processing symbolic quantities more strongly activates a pathway that does not rely on this intermediate number-sensitive processing stage.

Our results show an anatomical distinction between the number-sensitive and number-selective cortical regions. Experiment 1 shows number-sensitive processing in superior parietal cortex. Contrary, the IPS activation in the conjunction of symbolic and nonsymbolic quantities in Experiment 2 was located more anteriorly, at a location that corresponds with activity observed in experiments that specifically investigated number-selective coding (Piazza et al. 2004, 2007; see Fig. 5*A,B*). An analogous distinction between number-sensitive and number-selective processing has also been found in electrophysiological experiments in monkeys. Whereas number-sensitive neurons have been found in area LIP (Roitman et al. 2007), number-selective neurons are traditionally found more anteriorly in the IPS (Nieder and Miller 2004). Such a posterior to anterior gradient along the occipitoparietal visual stream from number-sensitive to number-selective processing is consistent with our results from the number-selective areas analysis showing that number-sensitive processing is an intermediate processing step in nonsymbolic number processing between early visual sensory analysis and a number-selective coding system.

As the present study shows, a combination of a classic statistical parametric mapping approach and connectivity analyses provides an interesting vantage point to interpret functional brain images and can be an efficient tool to validate models of cognitive functioning. Although this approach is already

established in other domains, the present study is to our knowledge the first to investigate brain connectivity during number processing. Nevertheless, some questions remain for future research. The first question relates to the fact that the paths in our number-selective areas analysis do not necessarily represent anatomical connections in the human brain. In Experiment 2, the modeling of brain activation using number-selective areas provides evidence for effective connectivity between areas under different conditions, without direct anatomical assumptions about connectivity. It is possible, for example, that occipital visual areas contact IPS only indirectly when processing symbolic stimuli. Cohen and Dehaene (1991) reasoned that a neural system must exist that identifies numerical symbols and their relative position in a stimulus. Analogous to the visual word form (Warrington and Shallice 1980), they termed the representation resulting from this system the visual number form and argued that it is implemented in occipitotemporal areas (Dehaene and Cohen 1995; Cohen and Dehaene 1996). Because a precise anatomical or functional description of the number form is still lacking, it was not possible to include it in the number-selective areas analysis in the present study. This must be focused on in later studies. A second issue that deserves extra attention in future research relates to hemispheric specialization for number processing. In Experiment 2, we observed shared activation for symbolic and nonsymbolic stimuli in the left but not in the right IPS. We therefore restricted the number-selective areas analyses to the left hemisphere. Although number-related activity is commonly found in both hemispheres, previous work discussed the possibility that during development, the left IPS develops a more fine-tuned shared representation for symbolic and nonsymbolic quantities than the right IPS (Piazza et al. 2007; Ansari 2008). However, additional evidence that the left and right hemispheres differentially process numerical information is still needed before strong conclusions can be drawn. We believe that the combination of localization and connectivity studies on functional brain data will aid in clarifying these issues and in enhancing our understanding of how the brain processes numbers in general.

Supplementary Material

Supplementary material can be found at: http://www.cercor.oxfordjournals.org/

Funding

Ghent University Research Council (BOF; 01J01406 to S.S.); Belgian Science Policy, Interuniversity Attraction Poles program (P6/29) (to C.R.); Ghent University, GOA program; Ghent University BOF/GOA (BOF08/GOA/011 to T.V. and W. F.).

Notes

Conflict of Interest: None declared.

Address correspondence to Chantal Roggeman, Department of Experimental Psychology, Ghent University, Henri Dunantlaan 2, B-9000 Ghent, Belgium. Email: chantal.roggeman@ugent.be.

References

Ansari D. 2008. Effects of development and enculturation on number representation in the brain. Nat Rev Neurosci. 9:278–291.

Badets A, Andres M, Di Luca S, Pesenti M. 2007. Number magnitude potentiates action judgements. Exp Brain Res. 180:525–534.

Behrens TEJ, Jenkinson M, Robson MD, Smith SM, Johansen-Berg H. 2006. A consistent relationship between local white matter architecture and functional specialisation in medial frontal cortex. Neuroimage. 30(1):220–227.

Bisley JW, Goldberg ME. 2003. Neuronal activity in the lateral intraparietal area and spatial attention. Science. 299:81–85.

Brannon EM. 2006. The representation of numerical magnitude. Curr Opin Neurobiol. 16:222–229.

Büchel C, Friston KJ. 1997. Modulation of connectivity in visual pathways by attention: cortical interactions evaluated with structural equation modelling and fMRI. Cereb Cortex. 7:768–778.

Buckley PB, Gillman CB. 1974. Comparisons of digits and dot patterns. J Exp Psychol. 6:1131–1136.

Buckner RL, Goodman J, Burock M, Rotte M, Koutstaal W, Schacter D, Rosen B, Dale AM. 1998. Functional-anatomic correlates of object priming in humans revealed by rapid presentation event-related fMRI. Neuron. 20:285–296.

Burock MA, Buckner RL, Woldorff MG, Rosen BR, Dale AM. 1998. Randomized event-related experimental designs allow for extremely rapid presentation rates using functional MRI. Neuroreport. 9:3735–3739.

Buschman TJ, Miller EK. 2007. Top-down versus bottom-up control of attention in the prefrontal and posterior parietal cortices. Science. 315:1860–1862.

Cantlon JF, Brannon EM, Carter EJ, Pelphrey KA. 2006. Functional imaging of numerical processing in adults and 4-y-old children. PLoS Biol. 4(5):844–854.

Christensen R. 2002. Plane answers to complex questions: the theory of linear models. New York: Springer. p. 473.

Cohen L, Dehaene S. 1991. Neglect dyslexia for numbers—a case-report. Cogn Neuropsychol. 8:39–58.

Cohen L, Dehaene S. 1996. Cerebral networks for number processing: evidence from a case of posterior callosal lesion. Neurocase. 2:155–173.

Cohen Kadosh R, Lammertyn J, Izard V. 2008. Are numbers special? An overview of chronometric, neuroimaging, developmental and comparative studies of magnitude representation. Prog Neurobiol. 84(2):132–147.

Connolly JD, Goodale MA, Menon RS, Munoz DP. 2002. Human fMRI evidence for the neural correlates of preparatory set. Nat Neurosci. 5(12):1345–1351.

Dale AM. 1999. Optimal experimental design for event-related fMRI. Hum Brain Mapp. 8:109–114.

Dale AM, Buckner RL. 1997. Selective averaging of rapidly presented individual trials using fMRI. Hum Brain Mapp. 5:329–340.

Dehaene S, Changeux JP. 1993. Development of elementary numerical abilities: a neuronal model. J Cogn Neurosci. 5(4):390–407.

Dehaene S, Cohen L. 1995. Towards an anatomical and functional model of number processing. Math Cogn. 1:83–120.

Dehaene S, Dehaene-Lambertz G, Cohen L. 1998. Abstract representation of numbers in the animal and human brain. Trends Neurosci. 21:355–361.

Dehaene S, Piazza M, Pinel P, Cohen L. 2003. Three parietal circuits for number processing. Cogn Neuropsychol. 20:487–506.

Denys K, Vanduffel W, Fize D, Nelissen K, Peuskens H, Van Essen D, Orban GA. 2004. The processing of visual shape in the cerebral cortex of human and nonhuman primates: a functional magnetic resonance imaging study. J Neurosci. 24(10):2551–2565.

Feigenson L, Dehaene S, Spelke E. 2004. Core systems of number. Trends Cogn Sci. 8(7):307–314.

Friston KJ, Penny WD, Glaser DE. 2005. Conjunction revisited. Neuroimage. 25:661–667.

Goldberg ME, Bisley J, Powell KD, Gottlieb J, Kusunoki M. 2002. The role of the lateral intraparietal area of the monkey in the generation of saccades and visuospatial attention. Ann NY Acad Sci. 956:205–215.

Gottlieb J. 2007. From thought to action: the parietal cortex as a bridge between perception, action, and cognition. Neuron. 53:9–16.

Grill-Spector K, Kushnir T, Edelman S, Itzchak Y, Malach R. 1998. Cue-invariant activation in object-related areas of the human occipital lobe. Neuron. 21:191–202.

Halgren E, Mendola J, Chong CDR, Dale AM. 2003. Cortical activation to illusory shapes as measured with magnetoencephalography. Neuroimage. 18(4):1001–1009.

Klein JC, Behrens TEJ, Robson MD, Mackay CE, Higham DJ, Desmond J, Johansen-Berg H. 2007. Connectivity-based parcellation of human cortex using diffusion MRI: establishing reproducibility, validity and observer independence in BA 44/45 and SMA/pre-SMA. Neuroimage. 34(1):204–211.

Koechlin E, Naccache L, Block E, Dehaene S. 1999. Primed numbers: exploring the modularity of numerical representations with masked and unmasked semantic priming. J Exp Psychol Human. 25(6):1882–1905.

Koyama M, Hasegawa I, Osada T, Adachi Y, Nakahara K, Miyashita Y. 2004. Functional magnetic resonance imaging of macaque monkeys performing visually guided saccade tasks: comparison of cortical eye fields with humans. Neuron. 41:795–807.

Lee KM, Wade AR, Lee BT. 2006. Differential correlation of frontal and parietal activity with the number of alternatives for cues choice saccades. Neuroimage. 33:307–315.

Maldjian JA, Laurienti PJ, Kraft RA, Burdette JH. 2003. An automated method for neuroanatomic and cytoarchitectonic atlas-based interrogation of fMRI data sets. Neuroimage. 19:1233–1239 (WFU Pickatlas, version X.xx).

Miezin FM, Maccotta L, Ollinger JM, Petersen SE, Buckner RL. 2000. Characterizing the hemodynamic response: effects of presentation rate, sampling procedure, and the possibility of ordering brain activity based on relative timing. Neuroimage. 11:735–759.

Moretto G, di Pellegrino G. 2008. Grasping numbers. Exp Brain Res. 188:505–515.

Murray SO, Schrater P, Kersten D. 2004. Perceptual grouping and the interactions between visual cortical areas. Neural Netw. 17: 695–705.

Nichols T, Brett M, Andersson J, Wager T, Poline JB. 2005. Valid conjunction inference with the minimum statistic. Neuroimage. 25:653–660.

Nieder A. 2005. Counting on neurons: the neurobiology of numerical competence. Nat Rev Neurosci. 6:1–14.

Nieder A, Freedman DJ, Miller EK. 2002. Representation of the quantity of visual items in the primate prefrontal cortex. Science. 297:1708–1711.

Nieder A, Miller EK. 2003. Coding of cognitive magnitude: compressed scaling of numerical information in the primate prefrontal cortex. Neuron. 37:149–157.

Nieder A, Miller EK. 2004. Analog numerical representations in rhesus monkeys: evidence for parallel processing. J Cogn Neurosci. 16(5):889–901.

Piazza M, Izard V, Pinel P, LeBihan D, Dehaene S. 2004. Tuning curves for approximate numerosity in the human intraparietal sulcus. Neuron. 44:547–555.

Piazza M, Pinel P, Dehaene S. 2007. A magnitude code common to numerosities and number symbols in human parietal cortex. Neuron. 53:293–305.

Reynvoet B, Brysbaert M, Fias W. 2002. Semantic priming in number naming. Q J Exp Psychol A. 55(4):1127–1139.

Roggeman C, Verguts T, Fias W. 2007. Priming reveals differential coding of symbolic and nonsymbolic quantities. Cognition. 105:380–394.

Roitman JD, Brannon EM, Platt ML. 2007. Monotonic coding of numerosity in macaque lateral intraparietal area. PLoS Biol. 5(8):1672–1682.

Seghier ML, Vuilleumier P. 2006. Functional neuroimaging findings on the human perception of illusory contours. Neurosci Biobehav Rev. 30:595–612.

Sereno MI, Pitzalis S, Martinez A. 2001. Mapping of contralateral space in retinotopic coordinates by a parietal cortical area in humans. Science. 294:1350–1354.

Simon O, Mangin JF, Cohen L, Le Bihan D, Dehaene S. 2002. Topographical layout of hand, eye, calculation and language dependent areas in the human parietal lobule. Neuron. 33:475–487.

Stevens M, Lammertyn J, Verbruggen F, Vandierendonck A. 2006. Tscope: A C library for programming cognitive experiments on the MS windows platform. Behav Res Methods. 38(2):280–286.

Todd JJ, Marois R. 2004. Capacity limit of visual short-term memory in human posterior parietal cortex. Nature. 428:751–754.

Tootell RBH, Hadjikhani N. 2001. Where is 'dorsalV4' in human visual cortex? Retinotopic, topographic and functional evidence. Cereb Cortex. 11:298–311.

Trick LM, Pylyshyn ZW. 1994. Why are small numbers enumerated differently? A limited-capacity preattentive stage in vision. Psychol Rev. 101(1):80–102.

Van Essen DC, Drury HA. 1997. Structural and functional analyses of human cerebral cortex using a surface-based atlas. J Neurosci. 17(18):7079–7102.

Verguts T, Fias W. 2004. Representation of number in animals and humans: a neural model. J Cogn Neurosci. 16(9):1493–1504.

Warrington EK, Shallice T. 1980. Word-form dyslexia. Brain. 103:99–112.